Available online at www.sciencedirect.com
SCIENCE DIRECT®

Journal of the European Ceramic Society 23 (2003) 2797–2803
www.elsevier.com/locate/jeurceramsoc

Progress in modelling of chemical-reaction limited wetting

O. Dezellus[1], F. Hodaj, N. Eustathopoulos*

LTPCM - UMR 5614 CNRS-INPG-UJF/ENSEEG, BP 75 Domaine Universitaire F—38402 Saint-Martin d'Hères Cedex, France

Abstract

In reactive metal/ceramic systems the wetting rate of small, millimeter sized droplets on smooth ceramic surfaces is controlled by the slower of two successive phenomena that intervene in the reaction process: diffusive transport of reacting species to or from the triple line, and local reaction kinetics at the triple line. The first case, of diffusive wetting, was modelled by Mortensen et al. [Scripta mater. 36 (1997) 645] a few years ago. The purpose of this paper is to present progress accomplished during the last few years in modelling the second type of wetting controlled by the reaction process at or close to the triple line. The predictions of equations derived from a model describing the change in contact angle and spreading rate with time are compared with experimental results obtained for different silicon alloys on carbon substrates.

Keywords: Contact angles; Interfaces; Reactivity; Spreading; Wetting

1. Introduction

Poor wetting is generally observed in non-reactive metal/ionocovalent oxide and metal/carbon systems. Indeed, in these systems the angle θ formed at the contact line of three phases, solid, liquid and vapour, is usually higher than ninety degrees.[2–4] Typical examples are the couples Cu/Al_2O_3 and Cu/C, for which the contact angle under high vacuum is as high as 120–140°.

A considerable improvement in wetting can be produced in such systems using certain alloying elements, which by reaction with the ceramic form a continuous layer of wettable compound along the metal/ceramic interface.

In view of the great interest expressed in brazing of ceramics and in electronic packaging, the dynamics of reactive wetting has been the subject of numerous studies published in recent years.[5–13] In non-reactive metal/metal or metal/ceramic systems, the time t_F for millimetre-sized molten droplets to reach capillary equilibrium is less than 0.1 s,[4,14] which is much shorter than the spreading times observed in reactive systems (typically 10–10^4 s). Starting from this observation, it was concluded in Ref. 8 that in reactive systems, the rate at which the droplet spreads is not limited by the viscous flow but by the rate of the interfacial reaction itself.

The rate of the interfacial reaction, in turn, may be controlled by the slower of two successive phenomena that intervene in the reaction process: diffusive transport of reacting species to or from the triple line and local reaction kinetics at the triple line.[8] In the first limit, diffusion is rate-limiting: local reaction rates are comparatively rapid, and the extent of local reaction which drives spreading is limited by the diffusive supply of reactant from the drop bulk to the triple line. Diffusion controlled wetting was modelled by Mortensen et al. a few years ago.[1] According to this model the rate of isothermal spreading is time-dependent and varies in direct proportion to angle θ. This dependence has been verified in the Cu–Cr [15] and Cu–Sn–Ti [16] alloys on vitreous carbon (C_v).

In the second case, with control by local reaction kinetics, the rate of reaction and hence the triple line velocity are expected to be constant with time.[8] This is confirmed by experiments: nearly constant triple line velocities $U = dR/dt$ (R being the drop base radius) have indeed been observed for a large part of the entire process in the CuSi/C system[17,18] (see Fig. 1a) and also for unalloyed aluminium on carbon for which diffusion clearly does not intervene.[8]

This paper focuses on this second type of control. The paper reviews the main results of studies performed on this subject by the Grenoble group during the last four

* Corresponding author. Tel.: +33-4-7682-6504; fax: +33-4-7682-6767.
E-mail address: nikos@ltpcm.inpg.fr (N. Eustathopoulos).
[1] Present address: Université Claude Bernard Lyon 1, UMR 5615 - LMI, Bât. Berthollet, 43 Bd. du 11 Novembre 1918, 69622 Villeurbanne Cedex France.

0955-2219/03/$ - see front matter © 2003 Elsevier Ltd. All rights reserved.
doi:10.1016/S0955-2219(03)00291-7

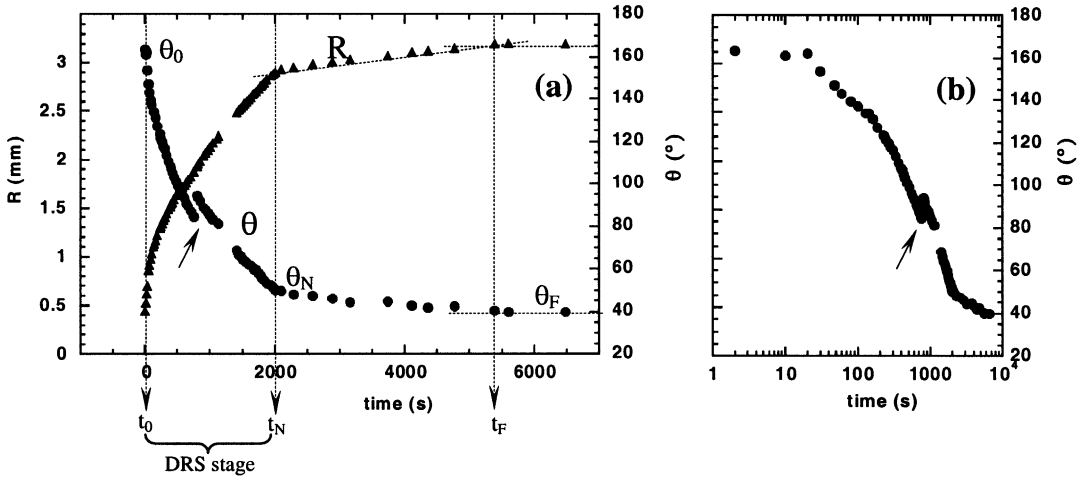

Fig. 1. (a) Time-dependent variation in drop base radius (R) and contact angle (θ) observed in the Cu–40 at.%Si/C_v system at 1180 °C. (b) Logarithmic representation of θ versus time. The arrows show the instant of detachment of the droplet from the capillary.

years. Particular emphasis is given to describe a model leading to analytical expressions of contact angle and drop base radius as a function of time. The predictions of the model will be compared to experimental results published previously as well as new ones obtained for various M–Si/C systems (with M = Cu, Ni, Ge). In these systems, above a certain value of Si mole fraction in the alloy,[19] silicon reacts with carbon, forming dense layers at the interface with submicrometer thickness of SiC.

Wetting results have been obtained by the "dispensed drop" method (derived from the classical sessile drop technique[4] Fig. 2) in a metallic furnace under a vacuum of 10^{-5} Pa. Experiments were carried out using millimeter-size droplets and smooth (average roughness of a few nanometers) vitreous carbon or pseudo-monocrystalline graphite[20] substrates. The metal–silicon alloys used were prepared from pure components (purity $\geqslant$99.997 wt.%) by melting and alloying in an alumina crucible during experiments performed in high vacuum (10^{-5} Pa). Once the experimental temperature is attained, the liquid is extruded from the crucible into a capillary and then the entire capillary introducer and the alloy droplet descend so as to initiate contact between the lower surface of the droplet and the C substrate. The capillary introducer then rises again and this movement induces complete transfer of the drop to the C substrate (Fig. 2).

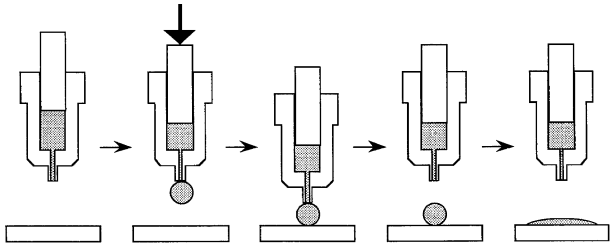

Fig. 2. Schematic presentation of the "dispensed drop" method.

2. Characteristic contact angles

The first stage in modelling reactive spreading is to determine the meaning of the initial and final contact angles. This is necessary to define the driving force for spreading.

A plot of the variation of contact angle θ and droplet base radius R versus time for an experiment conducted at 1180 °C for a Cu-40 at.%Si alloy by the dispensed drop technique is given in Fig. 1a. The perturbation on the $\theta(t)$ curve at $t\approx750$ s is due to a slight increase in drop volume from fresh liquid contained in the crucible at the moment of drop separation from the capillary. This increase occurs at constant drop base radius.

Spreading occurs between $\theta = 180°$ and a final or steady contact angle θ_F, which is close to 40°. The spreading regime between 180° and the first measured contact angle of about 160°, noted θ_0, is too fast to be followed by the CCD camera used in this study. In other words, the time t_0 corresponding to θ_0 is different from but very close to zero.

Because of the rapid change in contact angle during the very first moments of wetting, more accurate determination of the initial contact angle θ_0 is possible using a logarithmic scale for time t. An example of $\theta(\log t)$ curve is given in Fig. 1b. When the time tends towards zero, the contact angle tends towards a constant value θ_0 close to 160°. This contact angle is identified as the contact angle of molten silicide on the *unreacted* C_v substrate.

To verify this hypothesis, the θ_0 values for several reactive CuSi alloys, (which are alloys containing more than 15 at.% Si)[19] are plotted on Fig. 3 as a function of mole fraction of Si. All θ_0 values are close to 150–160°, whatever the composition of the alloy. According to the above interpretation of θ_0, if a non-reactive alloy is used, the steady-state contact angle would be close to

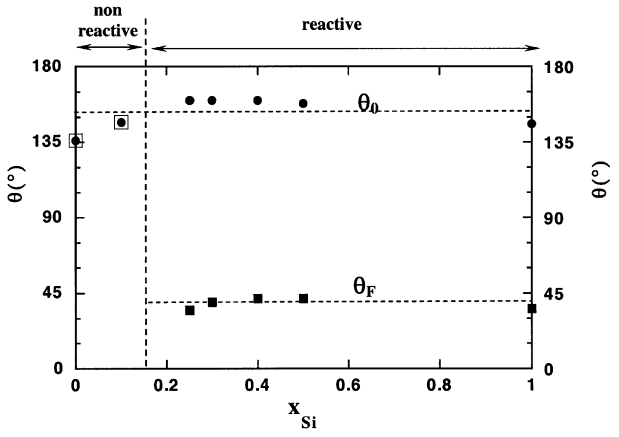

Fig. 3. Variation of initial contact angle θ_0 (•) and final contact angle θ_F (□ and ■) as a function of Si mole fraction. Cu–Si/C_v couples at $T=1200$ °C except for pure Si ($T=1420$ °C).

the plateau value. This was confirmed by results obtained with a Cu-10 at.%Si alloy for which the initial contact angle θ_0 is also close to 150°. But contrary to the reactive alloys, this angle remains constant with time ($\theta_F=\theta_0$).

The results of Fig. 3 clearly show that in the CuSi/C_v system the transition from non-wetting to wetting corresponds to the transition from non-reactive to reactive alloys. As this figure shows, in the non-reactive range, the addition of Si to Cu not only does not decrease the contact angle of copper on C_v, but it causes a significant increase, about 20°, in this value. In other words, Si does not adsorb at Cu/C_v interface, i.e. it is not *active* at this interface.

Thus, in this system, the low final contact angles observed experimentally in the reactive range are due *only* to reaction, (i.e. to the formation of wettable SiC),[21] and not to adsorption.

From this discussion, it can be concluded that the chemical affinity of an alloying element for a substrate (as that of silicon for carbon) does not necessarily imply that this element is active at the alloy/substrate interface. For this reason, theories that try to explain reactive wetting *only* by adsorption are incomplete.

3. Kinetic stages controlled by the interfacial reaction

On the $R(t)$ curve between $t_0\approx0$ and t_F two kinetic stages can be defined (Fig. 1a). In the first stage ($t_0 < t < t_N$, where t_N denotes the contact angle θ_N at which the sharp change in the slope of R versus t curves occurs—see Fig. 1), the spreading rate $U=dR/dt$ decreases *continuously* with time, first rapidly, then much more slowly, thus justifying why this part of the curve was called "linear spreading".[8] However, even in this part of the spreading process U varies by up to a factor two (Fig. 4). For this reason, spreading between t_0 and t_N, is called decreasing rate spreading (DRS).[21]

In contrast to the first stage in Fig. 1, the second stage (between t_N and t_F) is strictly linear. This stage, during which the change in contact angle is very limited (about 10°), takes place at a spreading rate one order of magnitude lower than in DRS stage. The transition between the DRS and linear stages is abrupt. Similar spreading curves were obtained for other silicon alloys and for pure Si. In all cases a final, strictly linear spreading follows a first stage of comparatively rapid spreading with a time-dependent triple line velocity. The origin of the final constant rate spreading will be discussed in a future paper. In the next section, modelling of the main reactive stage, DRS, described in details in Ref. 21, will be presented. Moreover an extension of the analysis given in Ref. 21 will be done in order to relate the kinetic constant of the wetting process to the kinetic constant and to the driving force of the chemical reaction that controls the wetting rate.

4. Modelling

In Ref. 8, it was assumed that during the initial stage of wetting the instantaneous contact angle lies between two limits: an upper limit, which is the contact angle on the unreacted substrate, and a lower limit which is the equilibrium contact angle θ_e on a substrate only partially transformed to the reaction product. In the present study, it is assumed that, at any time between t_0 and t_N, i.e. during the entire DRS stage, the instantaneous contact angle is higher than *but very close* to this equilibrium contact angle ($\theta\approx\theta_e$).

For the case of uniform dispersion of a particle phase P (in this case P is SiC) on a substrate S (here S is C_v), θ_e is given by the Cassie equation:[22]

$$\cos\theta_e = \alpha.\cos\theta_P + (1-\alpha).\cos\theta_S \quad (1)$$

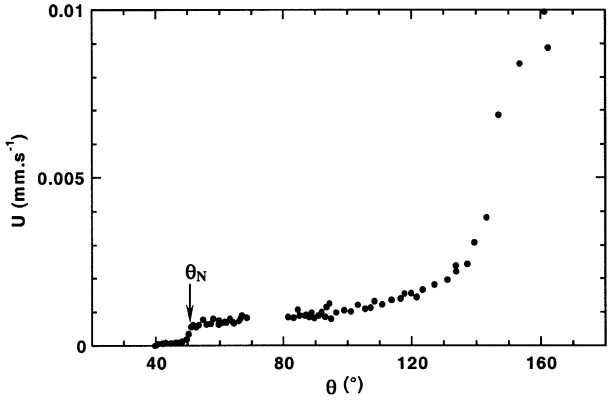

Fig. 4. Variation of triple line velocity (U) with instantaneous contact angle θ for the Cu–40 at.%Si/C_v system at 1180 °C. The arrow indicates the contact angle θ_N at which the sharp change in the slope of R versus t curves occurs (see Fig. 1).

In Eq. (1), α is the surface coverage of the discontinuous phase (SiC); θ_P and θ_S are the equilibrium contact angles of liquid on SiC and C, respectively with $\theta_P \approx \theta_F$ and $\theta_S \approx \theta_0$.

In the present case, the reacted interface is not a uniform dispersion of SiC particles; even after a few seconds of contact between the alloy and C_v this interface is completely covered by SiC except in the vicinity of the triple line where a *mixed zone* with α less than one appears[21] (Fig. 5). Inside this zone α is defined as $\alpha = 1 - S_C/S$ where S is the total surface area of the mixed zone and S_C is the part of S not covered by the reaction product. The width L of this mixed zone, as estimated by experiments involving the advancing and receding of the triple line and by characterisation of quenched samples, may reach a few tens of μm at the beginning of spreading ($\theta \approx 150°$) but decreases rapidly with time towards micron and eventually submicron sizes.[21]

Using Eq. (1) for interpreting the $\theta(t)$ curves means that the instantaneous contact angle at any time $t_0 < t < t_N$ is close to the equilibrium contact angle on a composite surface with the surface coverage $\alpha(t)$ [i.e. $\theta(t) = \theta_e\{\alpha(t)\}$]. Consequently, the time-dependent rate of change of θ, $\frac{d\theta}{dt}$, is fixed by the time-dependent change of α, $\frac{d\alpha}{dt}$:

$$\frac{d\theta}{dt} = -\frac{(\cos\theta_F - \cos\theta_0)}{\sin\theta} \cdot \frac{d\alpha}{dt} \quad (2)$$

In order to calculate $\frac{d\alpha}{dt}$, one more hypothesis must be made on the process limiting the reaction rate in the *mixed zone*. This may be one of the following phenomena, dissolution of carbon into the alloy (i.e. transfer of C atoms, at the C_v/alloy interface, from vitreous carbon to the melt), diffusion of carbon atoms from the dissolved area to the growing SiC/alloy interface and attachment kinetics at this interface (i.e. transfer of Si and C from the melt to the growing SiC crystal).

Limitation by liquid state diffusion of carbon or by the process of atom attachment at the growing interface would lead to a spreading rate independent of the carbon substrate structure. However it was found that the spreading rate in the DRS stage on monocrystalline graphite is lower by a factor 5 than the spreading rate on C_v.[23] Therefore, spreading kinetics is not limited by the liquid state diffusion or by the process at the growth interfaces but by the process at the dissolution interface. Under these conditions the rate of reduction of the metal/carbon interface in the mixed zone is proportional to the area not covered by the reaction product:

$$\frac{dS_C}{dt} = -kS_C \quad (3)$$

where k is a constant in s^{-1}.

Assuming the mixed zone area S remains constant during spreading, the above equation is transformed to:

$$\frac{d\alpha}{dt} = k(1-\alpha) \quad (4)$$

The approximation $S \approx 2\pi RL \approx$ constant allows analytical expressions of spreading rate to be obtained. Actually, during spreading, S can vary because both R and L vary (R increases and L is expected to decrease). The error made on k due to the approximation $S \approx$ constant obtained by considering that R increases at $L \approx$ constant (evaluated a posteriori, using experimental results) is, on average, about 50%. However, as L does decrease, the final error on k would be lower than 50%.

The constant k of Eq. (3) can be related to the kinetic constant of the dissolution process k_d and to the driving force of the dissolution process by equating the dissolving flux of carbon (in mol s^{-1}) to the flux of C participating in SiC growth:

$$k = k_d \frac{V^m_{SiC}}{f.e}\left[\mu_C^{C/L} - \mu_C^{L/C}\right] \quad (5)$$

where V^m_{SiC} is the molar volume of SiC, e is the average thickness of the reaction layer in the mixed zone and f a geometrical factor taking into account the details of the configuration in the mixed zone i.e., the shape of reaction product dendrites (f is in the order of unity). $\mu_C^{C/L}$ is the chemical potential of carbon on the solid side of the interface ($\mu_C^{C/L} = \mu_C^D$, where D corresponds to the metastable equilibrium between C and liquid, Fig. 6) and $\mu_C^{L/C}$ is the chemical potential of carbon in the liquid alloy at the carbon/liquid interface.

As the overall process is limited by the process at the dissolving interface, the chemical potential $\mu_C^{L/C}$ is fixed by the equilibrium of formation of reaction product SiC:

$$((Si))_M + ((C))_M \rightarrow SiC \quad (6)$$

Therefore $\mu_C^{L/C} \approx \mu_C^E$ (Fig. 6). For calculating the driving force $\Delta\mu = \mu_C^{C/L} - \mu_C^{L/C} = \mu_C^D - \mu_C^E$ the conditions of equilibrium for reaction (6) are written for points E and I, where I corresponds to the equilibrium of three phases, C, SiC and liquid. It yields:

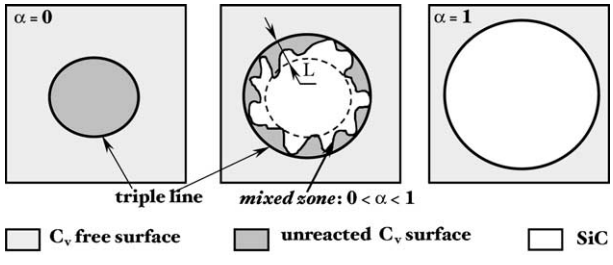

Fig. 5. Schematic presentation of the reacted interface during spreading, defining the *mixed zone* of width L where the surface coverage α is less than unity.

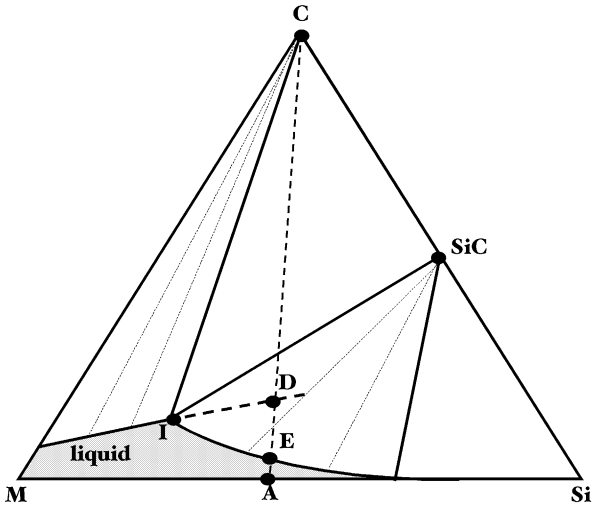

Fig. 6. Schematic isothermal section of the M–Si–C ternary system.

$$\Delta\mu = \mu_C^D - \mu_C^E = \mu_{Si}^E - \mu_{Si}^I = RT\ln\left(\frac{a_{Si}^E}{a_{Si}^I}\right) \approx RT\ln\left(\frac{a_{Si}}{a_{Si}^I}\right) \quad (7)$$

As the solubility of carbon in liquid M–Si (M = Cu, Ni, Ge) is low (< 1 at.%C) silicon activity in the ternary liquid alloy M–Si–C, a_{Si}^E, is nearly equal to a_{Si} corresponding to the binary M–Si alloy (point A, Fig. 6). a_{Si} is calculated from Refs. 24–26. a_{Si}^I depends only on temperature and can be calculated from the value of the Gibbs energy of formation of SiC from pure molten Si and solid C, $\Delta G_f^0(T)$: $a_{Si}^I = \exp\left(\frac{\Delta G_f^0(T)}{RT}\right)$. The value $\Delta G_f^0(T) = -113482 + 37.4872\ T$ (in Joule) is the mean of the values given by Kubaschewski and Alcock[27] and by Sambasivian et al.[28]

By combining Eqs. (5) and (7) we obtain:

$$k = k_d \frac{V_{SiC}^m}{f.e} RT\ln\left(\frac{a_{Si}}{a_{Si}^I}\right) \quad (8)$$

In the framework of this model, the parameter k in Eq. (4) is taken as a constant at fixed T and a_{Si}. By combining Eqs. (2) and (4) the following expression of $\frac{d\theta}{dt}$ is derived:

$$\frac{d\theta}{dt} = -\frac{k}{\sin\theta}(\cos\theta_F - \cos\theta) \quad (9)$$

which after integration yields:

$$\cos\theta_F - \cos\theta = (\cos\theta_F - \cos\theta_0).\exp(-k\ t) \quad (10)$$

According to this expression, logarithmic plots of $\cos\theta_F - \cos\theta$ versus time would be linear with a slope equal to minus k.

Fig. 7 shows the logarithmic plot of $\cos\theta_F - \cos\theta$ as a function of time for Cu–40 at.%Si alloys on C_v at different temperatures. A difficulty with this representation appears at the high contact angle range due to the perturbation of $\theta(t)$ curves occurring in the dispensed drop technique during drop detachment from the capillary. During this detachment the contact angle increases sharply, as explained elsewhere,[15] which leads to translation of the straight line towards higher values. However the slopes of the straight lines before and after detachment must be the same, as indeed observed experimentally in Fig. 7 for the experiment at 1150 °C. (For the other temperatures and for the sake of clarity, only the results after drop detachment are considered). It must be noted that, in order to draw the straight line, a value must be chosen for θ_F. For the Cu–40 at.%Si alloy the value $\theta_F = 35°$ was used, regardless of the temperature, because the effect of temperature on the final contact angle in this type of systems is very weak (about 1 degree per 100 °C).[29]

According to Eq. (8), the kinetic constant k_d can be calculated from the value of k if the driving force of the dissolution process $\Delta\mu$ [Eq. (7)] can be evaluated and the thickness e of the reaction product near the triple line is known. For the Cu–40 at.%Si alloy at $T = 1180$ °C, the constant k obtained from the slope of the straight line is $k = 1.3\times10^{-3}$ s^{-1}. For this alloy $e \approx 150$ nm,[21] $a_{Si} = 0.32$, $a_{Si}^I = 7.6\times10^{-3}$ and $V_{SiC}^m = 1.25\times10^{-5}$ m^3 mol^{-1} [30] leading, for $f = 1$, to $k_d \approx 4\times10^{-10}$ mol m^{-2} s^{-1}. Taking into account the experimental errors and the uncertainties on the factor f, the k_d value is given within a factor 5. This example illustrates how the study of reactive spreading allows to obtain the order of magnitude of kinetic constant of dissolution of a solid, a quantity which can hardly be measured by other methods.

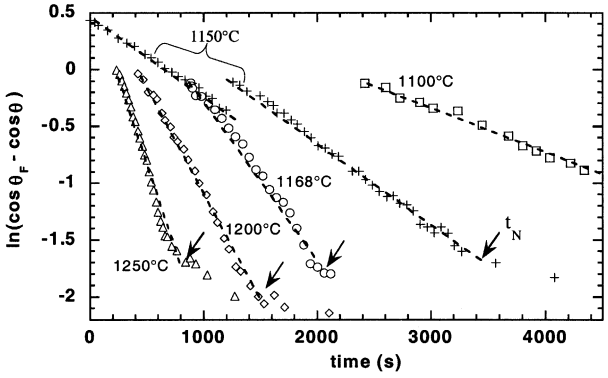

Fig. 7. Napierian logarithm of $\cos\theta_F - \cos\theta$ versus time for Cu–40 at.%Si alloy/C_v system at different temperatures. The arrows show the time t_N at which the sharp change in the slope of R versus t curves occurs (see Fig. 1a).

The spreading rate $U = \frac{dR}{dt}$ is calculated from Eq. (10) taking the volume V of the droplet to be constant, i.e. assuming that the thickness of the reaction product is much lower than the droplet size:

$$\frac{U}{F(\theta)} = k\left(\frac{3V}{\pi}\right)^{1/3}(\cos\theta_F - \cos\theta) \quad (11)$$

with:

$$F(\theta) = -\frac{\cos\theta\left(2 - 3\cos\theta + \cos^3\theta\right) - \sin^4\theta}{\sin\theta\ (2 - 3\cos\theta + \cos^3\theta)^{4/3}} \quad (12)$$

Contrary to Eq. (10), verification of Eq. (11) by plotting the spreading rate $U = \frac{dR}{dt}$ divided by $F(\theta)$ versus the cosine of the instantaneous contact angle, predicted to yield a straight line, does not need the value of θ_F. Moreover as the detachment of the droplet from the capillary disturbs the $R(t)$ curves much less than the $\theta(t)$ curves, presentation of experimental results on the basis of Eq. (11) provides a means of discussing the validity of the model for the high contact angle–short spreading times range.

Fig. 8 presents an example for the Ni–63 at.%Si couple. The experimental data agree with the linearity predictions of Eq. (11) in a large domain of θ lying between $\theta_N \approx 50°$ and $\theta \approx 130°$. Extrapolation to zero spreading rate leads to $\theta_F = 30°$ which is in agreement with the contact angles measured on SiC with non-reactive Ni–Si alloys.[29] For contact angles $\theta > 130°$ the spreading rate deviates strongly from linearity and this behaviour was verified for all alloys used in this study.

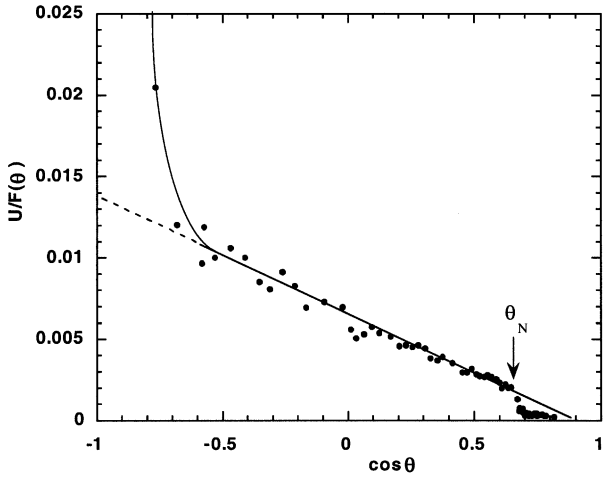

Fig. 8. Experimental results of spreading rate $U(\theta)$ divided by the function $F(\theta)$ [see Eq. (11)] versus the cosine of contact angle for the Ni–63 at.%Si alloy/C_v system at 1202 °C. The arrows indicate the contact angle at which the sharp change in the slope of R versus t curves occurs (see Fig. 1a).

A possible reason for this deviation is that during the first moments of spreading a steady configuration at the substrate/alloy interface close to the triple line is not yet established. This interpretation is reinforced by the fact that a microstructural transition of reaction product at the interface from predominantly equiaxial (at the center of the drop) to predominantly columnar microstructure to the periphery occurs around 130°.[21]

For evaluating the activation energy of reactive spreading in the range $\theta < 130°$, the constant k is first determined for different alloys and experimental temperatures explored in this study from the slope of straight lines such as those of Fig. 7.

Then, in order to obtain the true activation energy of the dissolution process, the logarithm of constant k divided by the driving force $\Delta\mu$ is plotted as a function of $1/T$ for different silicon alloys (Fig. 9). This assumes that all the other quantities (V^m_{SiC}, e) and factors (f) do not vary significantly with T.

The results show a limited but significant effect of Si activity on the value of the pre-exponential factor of k_d. Note that for Ni–63 at%Si and Cu–50 at%Si alloys for which a_{Si} is nearly the same, the experimental points belong to the same straight line. An effect of a_{Si} on the activation energy E_a is difficult to deduce and the value $E_a \approx 290$ kJ mol^{-1} can represent all results.

A better evaluation of E_a would be possible if, for each alloy, the change with T of reaction product thickness e in the vicinity of the triple line was known.

A systematic determination of e has not been performed[31] but it has been found that an increase in T of 250 °C causes an increase in e by a factor, which would be at most equal to 10. Such an effect of T on e would increase the activation energy by about 30%.

Therefore, the activation energy of dissolution of vitreous carbon in different silicon alloys is in the range

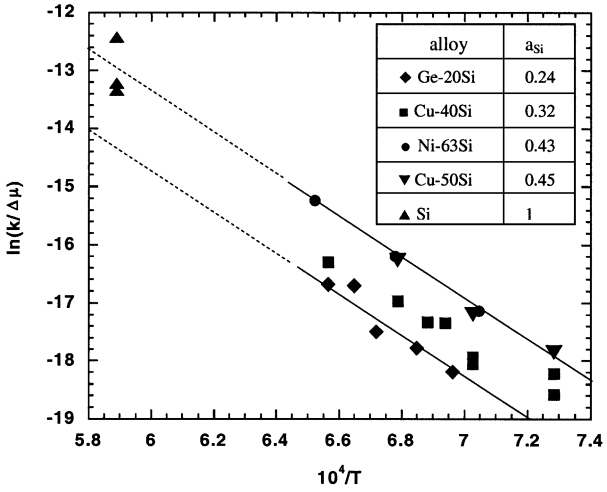

Fig. 9. Arrhenius plot of the reduced kinetic constant of dissolution $k/\Delta\mu$ [see Eqs. (7) and (8)] for different silicon alloys. k is in s^{-1}, T is in degrees K. The alloy compositions are given in at.%Si.

300–400 kJ mol^{-1}. For pseudo-monocrystalline graphite E_a is increased by a factor 1.5.[31] Such a value is one order of magnitude higher than the activation energies of diffusion in metallic melts (a few tens of kJ mol^{-1}) which is consistent with the assumption of spreading not limited by liquid state diffusion. It has been proposed in Ref. 8 that the activation energy is mainly determined by the rupture of C–C chemical bonds at the substrate surface.

5. Conclusions

Equations describing spreading controlled by the local process at the triple line were recently derived on the basis of two assumptions: (i) at any time the instantaneous contact angle is greater than but very close to the equilibrium contact angle corresponding to the surface coverage of the reaction product in the vicinity of the triple line, and (ii) the reaction rate is controlled by the dissolution process i.e. by the process of atom transfer occurring at the substrate/alloy interface.

The analytical equation derived for the spreading rate dependence $U(\theta)$ is rather complex but indicates that the spreading rate varies roughly as the cosine of the instantaneous contact angle, with opposite sign. In contrast, a simple equation is derived for the $\theta(t)$ dependence, according to which the cosine of contact angle decreases exponentially with time between an initial value corresponding to the fully unreacted substrate and a final value corresponding to a substrate fully covered by the reaction product:

$$\cos\theta_F - \cos\theta = (\cos\theta_F - \cos\theta_0).\exp(-k\ t)$$

The constant k is proportional to the kinetic constant k_d and to the driving force of the dissolution process.

The model equations compared to experimental results obtained for different silicon alloys on carbon substrates show good agreement in a wide domain of contact angles except for high, non-wetting contact angles ($>130^\circ$) where the model equations lead to considerable underestimation of spreading rate. The activation energy of carbon dissolution in molten silicides is found to be close to 300 kJ mol^{-1} and it is nearly independent of the metal matrix (Cu, Ni or Ge) and of Si activity in the alloy.

To the authors' knowledge the above equation is the first proposed to describe spreading in reaction-limited wetting.

Acknowledgements

This work was in part supported by a NEDO International Research Grant (project "Wettability of Solids by Liquids at High Temperature") supervised by the Ministry of Economy, Trade and Industry of Japan.

References

1. Mortensen, A., Drevet, B. and Eustathopoulos, N., *Scripta Mater.*, 1997, **36**, 645.
2. Naidich, Y., *Progress in Surface and Membrane Science*. D. A. Cadenhead and J. F. Danielli. 1981, pp. 353, Acadamic Press, New-York.
3. Nogi, K., *Trans. JWRI*, 1993, **22**, 183.
4. Eustathopoulos, N., Nicholas, N. and Drevet, B., *Wettability at High Temperatures, Pergamon Materials Series*. Elsevier, Amsterdam, 1999.
5. Eustathopoulos, N. and Drevet, B., *J. Phys.*, 1994, **III**(4), 1865.
6. Landry, K., Rado, C., Voitovich, R. and Eustathopoulos, N., *Acta Mater.*, 1997, **45**, 3079.
7. Ambrose, J. C., Nicholas, M. G. and Stoneham, A. M., *Acta Metall. Mater.*, 1993, **41**, 2395.
8. Landry, K. and Eustathopoulos, N., *Acta Mater.*, 1996, **44**, 3923.
9. Meier, A., Chidambaram, P. R. and Edwards, G. R., *Acta Mater.*, 1998, **46**, 4453.
10. Saiz, E., Cannon, R. and Tomsia, A., *Acta Mater.*, 1998, **48**, 4449.
11. Yost, F. and O'Toole, E., *Acta Mater.*, 1998, **46**, 5143.
12. Warren, J., Boettinger, W. and Roosen, A., *Acta Mater.*, 1998, **46**, 3247.
13. Nomura, M., Iwamota, C. and Tanaka, S., *Acta Mater.*, 1999, **47**, 407.
14. Ebrill, N., Durandet, Y. and Strezov, L., *Trans JWRI*, 2001, **30**, 251.
15. Voitovitch, R., Mortensen, A., Hodaj, F. and Eustathopoulos, N., *Acta Mater.*, 1999, **47**, 1117.
16. Dezellus, O., Hodaj, F., Mortensen, A. and Eustathopoulos, N., *Scripta Mater.*, 2001, **44**, 2543.
17. Landry, K., Rado, C. and Eustathopoulos, N., *Met. Trans. A*, 1996, **27A**, 3181.
18. Dezellus, O., Hodaj, F., Eustathopoulos, N., *Proc. Int. Conf. High Temperature Capillarity*, Cracow, Poland, 1997, ed. Eustathopoulos N., Sobczak N., Cracow, 1998, 18.
19. Rado, C., Drevet, B. and Eustathopoulos, N., *Acta Mater.*, 2000, **48**, 4483.
20. Landry, K., Kalogeropoulou, S. and Eustathopoulos, N., *Mat. Sci. Engin.*, 1998, **A254**, 99.
21. Dezellus, O., Hodaj, F. and Eustathopoulos, N., *Acta Mater.*, 2002, **50**, 4741.
22. Cassie, A. B. D., *Discussion of the Faraday Society*, 1948, **3**, 11.
23. Dezellus, O., Hodaj, F. and Eustathopoulos, N., *Trans. of JWRI*, 2001, **30**, 75.
24. an May, S., *Z. Metallkunde*, 1986, **77**, 805.
25. Witusiewicz, V., Arpshofen, I. and Sommer, F., *Z. Metallkunde*, 1997, **88**, 866.
26. Olesinski, R. W. and Abbaschian, G. J., *Bull. Alloy Phase Diagrams*, 1984, **5**, 2.
27. Kubaschewski, O. and Alcock, G. B., *Metallurgical Thermochemistry*, 5th ed.. Pergamon Press, Oxford, 1979.
28. Sambasivan, S., Capobianco, C. and Petuskey, W. T., *J. Amer. Ceram. Soc.*, 1993, **76**, 397.
29. Rado, C., Kalogeropoulou, S. and Eustathopoulos, N., *Acta Mater.*, 1999, **47**, 461.
30. Brandes, E. A., Brook, G. B., ed., *Smithells Metals Reference Book*, 7th ed. Butterworth and Heinemann Publishers, 1992.
31. Dezellus, O., Thesis, Institut National Polytechnique de Grenoble (France), 2000.